

IAC-13-E2.3-19331

ENGINEERING DESIGN OF A LOW GRAVITY EXPERIMENT ONBOARD REXUS 16: CHEMICAL WAVE IN SORET EFFECT (CWIS)

Wassilis Tzevelecos
Microgravity Research Center, Belgium, wassilis88@yahoo.it

Mr. William Runge
Université Libre de Bruxelles, Belgium, wrunge@med.unc.edu
Mr. Valerio Cestrone
Italy, valeriocestrone@live.it
Mr. Luigi De Filippis
Italy, luigi.de_lippis@hotmail.com
Mr. Fabrizio Mancino
Italy, fabriziomancino@gmail.com
Mr. Santolo Manzone
Italy, santolo.manzone@gmail.com
Mr. Antonio Pugliese
Italy, antoniopugliese88@gmail.com
Mr. Olivier Desenfans
Université Libre de Bruxelles, Belgium desenfans.olivier@gmail.com
Dr. Quentin Galand
Université Libre de Bruxelles, Belgium qgaland@ulb.ac.be
Prof. Stefan Van Vaerenbergh
Université Libre de Bruxelles, Belgium svanvaer@ulb.ac.be

The purpose of this experiment, entitled Chemical Waves in Soret Effect (CWIS), is to visualize the chemical wave induced by the thermodiffusion of a binary liquid mixture. The chemical wave is a concentration front that rapidly propagates from the thermal boundaries of the liquid mixture, and which marks the beginning of the chemical sorting phenomenon called thermodiffusion, induced by an imposed thermal gradient. In order to eliminate the contribution of buoyancy and bulk convective fluid motion, this experiment takes advantage of the several minutes of milligravity provided by an Improved Orion sounding rocket, as a part of the REXUS 16 launch campaign. The launch vehicle will fly to an altitude of nearly 100km, with a number of experiments on-board, ending with an atmospheric re-entry and parachute recovery of the experimental modules. The REXUS/BEXUS programme is realised under a bilateral Agency Agreement between the German Aerospace Centre (DLR) and the Swedish National Space Board (SNSB). This team's experimental module, currently under development, uses a Fizeau interferometer to study the chemical wave in a small-volume mixture of water and ethylene glycol, taking advantage of the difference in the refractive indices of these two fluids, and the time-dependent nature of the thermodiffusion process. This paper presents the chemical, electrical, mechanical, and thermal systems being developed for this unique application. A particular focus in this paper is the Finite Element Analysis (FEA) of the payload, required to maximally isolate the payload from the rocket's vibrations, but the other systems are presented in some depth also. Finally, this paper will present some of the qualification tests for the hardware and software, conducted with the guidance of the European Space Agency, and on a pre-defined timeline dating back to original project proposal in mid-2012.

I. INTRODUCTION

Many phenomena in the life sciences behave differently in spaceflight compared to on earth, due to the unique nature of spaceflight with respect to parameters such as gravity, vacuum, and radiation. As such, spaceflight offers a unique opportunity to conduct scientific investigation that is not otherwise possible. This type of investigation, both in basic and applied sciences, is a critical mechanism for moving forward our understanding of the life sciences, and often leads to innovations that improve the lives, healthcare, and education of everyday people here on earth.

One example of a basic chemical process that spaceflight allows us to observe is thermodiffusion, also called Soret Effect, which describes diffusion-driven separation of a liquid mixture across a thermal gradient.

The underlying theoretical explanation for thermodiffusion is still actively debated,[3] but thermodiffusion and chemical mass transport may well be manifestations of the same underlying diffusion mechanism.[2] In any case, the Navier-Stokes equations give us an analytical solution for thermodiffusion as shown by Geelhoed,[7] and verified in experimentation by Eslamian.[4]

On earth, when a thermal gradient is present, the driving force for fluid motion is buoyancy, which arises due to gravity, and typically results in the rising of warm fluid and sinking of cooler fluid. In space, whether in microgravity or in milligravity, buoyancy is anticipated to play a secondary role compared to the influence of thermodiffusion.

This distinction is shown generally in Figure 1.

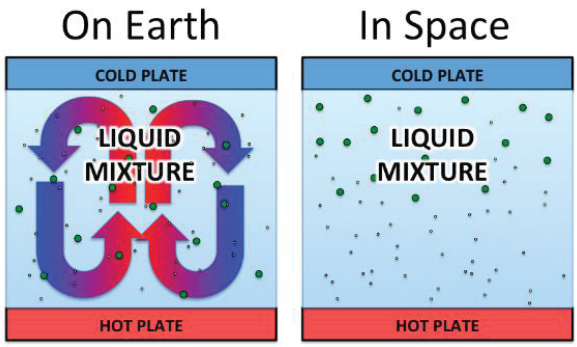

Fig. 1. Liquid behaviour in space vs. on earth

This document describes an experiment which is being developed to elucidate the early stages of the thermodiffusion process, by using a laser diagnostic technique called interferometry to assess the transient change in the refractive index of the mixture near the boundaries of the experimental cell. This differential refractive index across the thermal gradient arises due to the change in relative concentration of the two components (ethylene glycol and water) near the boundaries of the cell, due to the thermal gradient.

In binary mixtures a temperature gradient can work as a driving force for mass diffusion. Working from the general Navier-Stokes equations, this effect adds to the usual Fick's diffusion[7] and the balance equation of mass becomes:

$$\frac{\partial w}{\partial t} = D\nabla^2 w + DS_0(1-w_0)\nabla^2 T \qquad [1]$$

where,

w is the mass fraction of one component
D is the mass diffusivity
S_0 is the Soret coefficient
w_0 is the mean mass fraction
T is the local temperature

The mixture that will be used for the experiment is composed of water and ethylene glycol. This is important both for the time scale and the temperature constraints of the REXUS launch programme[5], and is contrasted with the efforts Eslamian[4] and others who have observed a similar phenomenon, largely in metals mixtures, as reflected in Figure 2. These previous studies, with the exception of Van Vaerenbergh's analytical study[11], which indicated the possibility of a chemical wave, have focused on the steady state diffusion coefficients, and experimental studies have suffered somewhat due to the influence of gravity. Still, it is clear from published data that there is a thermodiffusion process; what remains is to understand and characterize the transient effects.

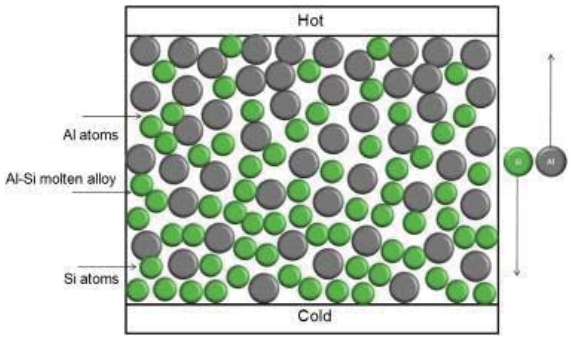

Fig 2. Eslamian's descriptive figure for thermodiffusion in a metal mixture

This project will present a combination of numerical and experimental results. These findings are expected to be relevant both to the basic understanding of thermodiffusion, and also to the many applications of this phenomenon. In particular, it is anticipated that thermodiffusion will prove relevant to crystal growth, chemical separation, chemical absorption/deposition, and possibly even macromolecule manipulation.

II. EXPERIMENT DESIGN

Chemical System

The liquid cell is the heart of the experiment. Here there are two chambers filled with liquids which will be studied during the course of the rocket flight. The first chamber is filled with pure ethylene glycol. The second chamber contains a mixture of 99% ethylene glycol with 1% distilled water by mass. The chamber of pure ethylene glycol will exhibit a change in refractive index due solely to thermal gradient. The experimental chamber with the binary mixture will exhibit a change in refractive index due both to temperature and the changing concentration gradient that is due to the Soret effect. Because the two liquids have approximately the same thermal characteristics, this allows us to isolate the contribution of the Soret effect to refractive index, and thus study the chemical wave due to the Soret effect.

Ethylene glycol was chosen on the basis of its ready availability, and relatively low melting point and high boiling point. It has seen use in motor vehicles as antifreeze, as well as on the Mir space station. It is not toxic to humans unless more than 1.4mL per kg of body weight is ingested.[9]

Mechanical System

In order to analyse the time-dependent thermodiffusion, and in particular the chemical wave, a Fizeau interferometer is used.

The Fizeau interferometer is the most commonly used interferometer for space-related instrumentation,[8] and allows for a very accurate and detailed characterization of the variation of refractive index throughout a material, including thermal variations.[10] This device, a combination of optics, a laser, and a camera, is used to develop a series of time-steps of fringe pattern images which will capture a change in the refractive index throughout the mixture, especially evident towards the hot boundary of the cell.

By analysing the fringe pattern images we will quantitatively and qualitatively assess the diffusion and separation of the water and ethylene glycol over the milligravity flight period of the REXUS rocket. The chamber with pure ethylene glycol will indicate the change in refractive index due solely to the thermal gradient. The chamber with the experimental mixture will indicate the change in refractive index due to both thermal gradient and diffusion, and having both sets of data allows us to isolate the change due to diffusion, and thus the Soret effect.

The liquid-containing cell is fixed to the optic plate, and bracketed on either side by a copper baseplate, as shown in Figure 3.

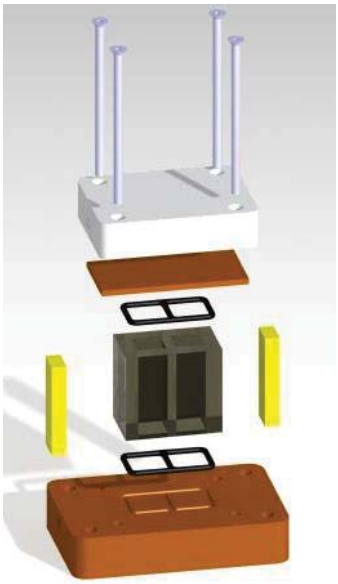

Figure 3. Experimental Cell Design

Each base has holes for two thermocouples to monitor temperature of the two chambers. Only the bottom plate is directly attached to the optic plate.

The copper base has two countersunk holes each for the two chambers, to accommodate the filling procedure for the cell. Each chamber has a pressure-compensating membrane on the bottom plate, which is necessary due to the changes in pressure and fluid volume as the rocket transitions from sea level, to 100k feet, and back to sea level.

The pressure compensation devices are put on the bottom plate because the chemical wave is occurring at the top plate. This pressure compensation system consists simply of an elastic membrane bound in place by Viton o-rings. Viton is a light-weight, flame-resistant fluoroelastomer with good electrical properties and acceptable shrinkage. It's usage dates back to the Apollo era.[1] The copper base and the top plate, made of teflon, are held together by four screws.

At the interface of the glass cell with the copper plate there is a gasket system of o-rings made of Viton, which is a material chosen mostly based on its safety with regards to the somewhat corrosive nature of the ethylene glycol.

The load-bearing between the two copper plates is achieved with four strong plastic columns. This is necessary because the glass cell itself is somewhat delicate and should not be a load-bearing member. The top teflon plate has four additional countersunk holes for the screws to fasten it to the bottom plate.

Optical System

The liquid-containing cell, depicted in Figure 4, is made of borosilicate. It has two chambers, to study the pure solution of ethylene glycol, and the liquid mixture of ethylene glycol and water, as detailed previously.

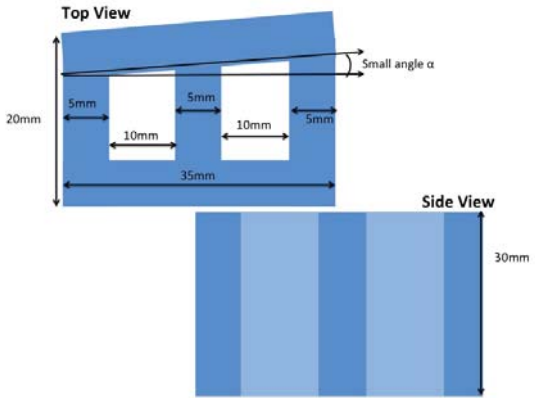

Figure 4. Experimental Cell Design

The height of the cell is 30mm. This value is constrained not only by the physical dimensions of the experiment module on-board the rocket, but also by the short duration of the milligravity period, and the need to

match the characteristic time of the chemical wave to the duration of our milligravity period.

The small angle, alpha, is explained in the next section, on the Laser System.

Laser System

The interferometer is used to assess the change in refractive index throughout both chambers of the cell. This interferometer is comprised of a laser, two collimators, a beam splitter and a lens to expand the beam.

The laser is a 45mW thermoelectrically cooled red laser system of 685 nm wavelength, manufactured by ONDAX. The layout of the complete optical system is depicted in Figure 5.

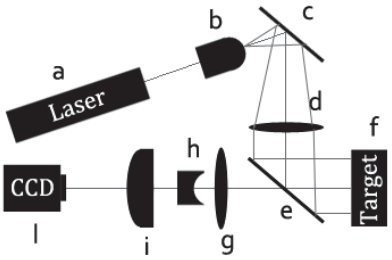

Figure 5. Optical System Layout

In Figure 5, (d) and (g) are converging spherical lenses, (h) and (i) are cylindrical lenses respectively diverging and converging one, (e) is a beam splitter, CCD is the charge-coupled device (camera) used to capture the interference pattern, (c) is a mirror, and (b) is an expanding lens. A Fizeau interferometer design was chosen because of the reduced planform area compared to a Mach-Zehnder interferometer and in particular to the resistance to vibration which characterize this application with sounding rocket.

For the functioning of the interferometer, the optical distance between the microscopic objective (b) and the lens (d) should be of its focal length in order to collimate the beam before that interference apply. What is particular in this system is the use of a not standard camera objective. This configuration was chosen because of its better resistance to shocks and also to apply image distortion in order to increase with cylindrical lenses the resolution along the thermal gradient of the Cell system.

Mechanical Layout

The overall mechanical design is shown in Figure 6. The top cover has been removed. The insulation between the module skin and the rocket skin is also not depicted. The significant components of the experiment are numbered 1-13. A legend is provided beneath the figure.

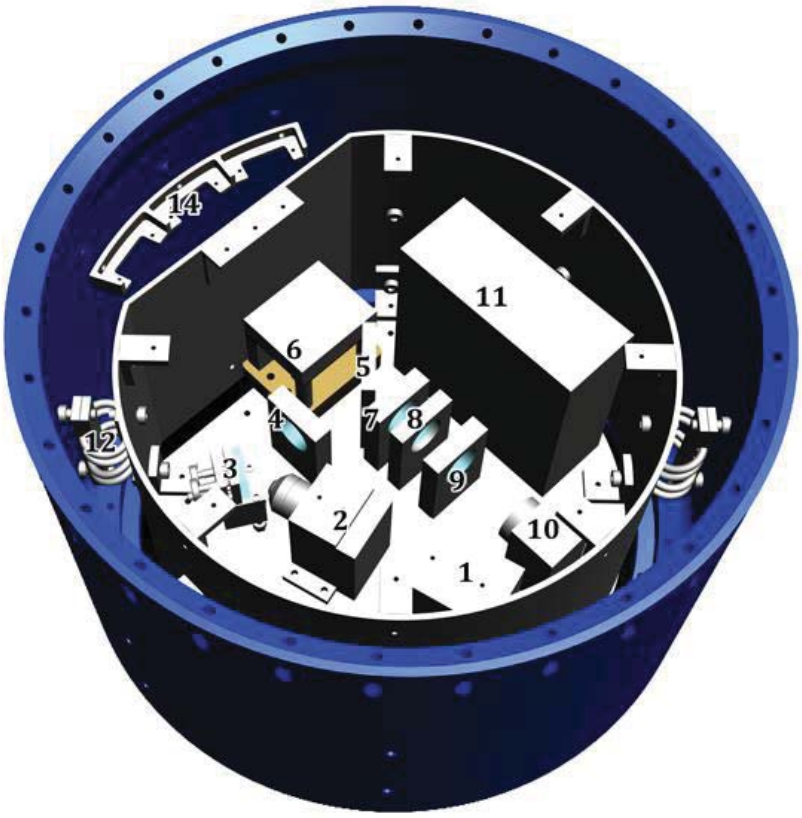

Figure 6. Component Layout

1. Laser
2. Microscopic Objective
3. Mirror
4. Collimating Lens
5. Beam Splitter
6. Liquid Cell system
7. Convergent Spherical Lens
8. First Cylindrical Lens
9. Second Cylindrical Lens
10. Camera
11. Electronics box
12. Dampers
14. Bracket for cable bypass

Structural Analysis

A structural analysis of the experimental module was carried out in FEMAPv10.3 for pre- and post-processing, with MD NASTRAN R3 as a processor. The bolts were modelled as rigid elements, in the Finite Element Model (FEM) RBE2 in the NASTRAN code.

Bolts were modelled as rigid elements in RBE2, and damping springs were modelled as Spring/Damper elements in the PBUSH code.

The components on the optical plate were modelled as mass elements, coded as CONM2 in NASTRAN. The optical plate itself, as well as the lateral skin, top cover, and L profiles were all modelled as plate elements. The assembled model, minus the top cover, is depicted in Figure 7.

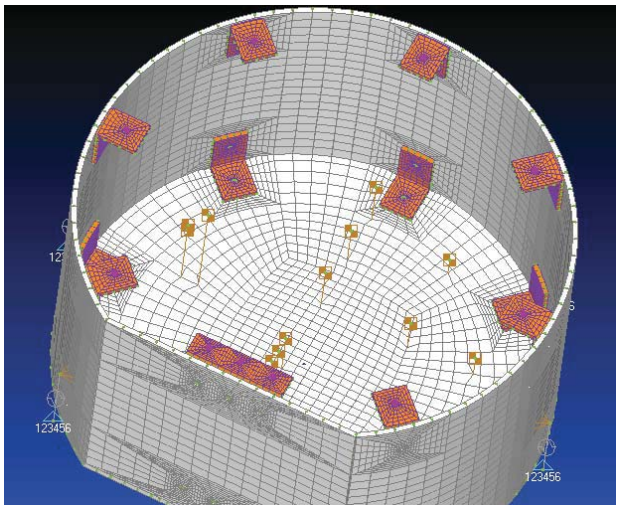

Figure 7. NASTRAN FEM model

The following pictures show the Von Mises stresses in contour. The loads were calculated for 20g vertical acceleration and 4 rad/s^2 angular acceleration. All components were modelled as 2024 aluminium. The various material parameters used in the FEM study are given in Table 1.

Parameter	Value
Young Modulus	7.308e+10 N/m
Poisson's Ratio	0.33
Tension Stress Limit	2.9e+8 N/m^2
Shear stress limit	1.67e+8 N/m^2
Density	2768 kg/m^3

Table 1: FEM Modelling Values

Figures 8 and 9 show the contours of the Von Mises stress for the complete module. The most highly stressed areas include the L-brackets and the mounting points for optics near the centre of the plate.

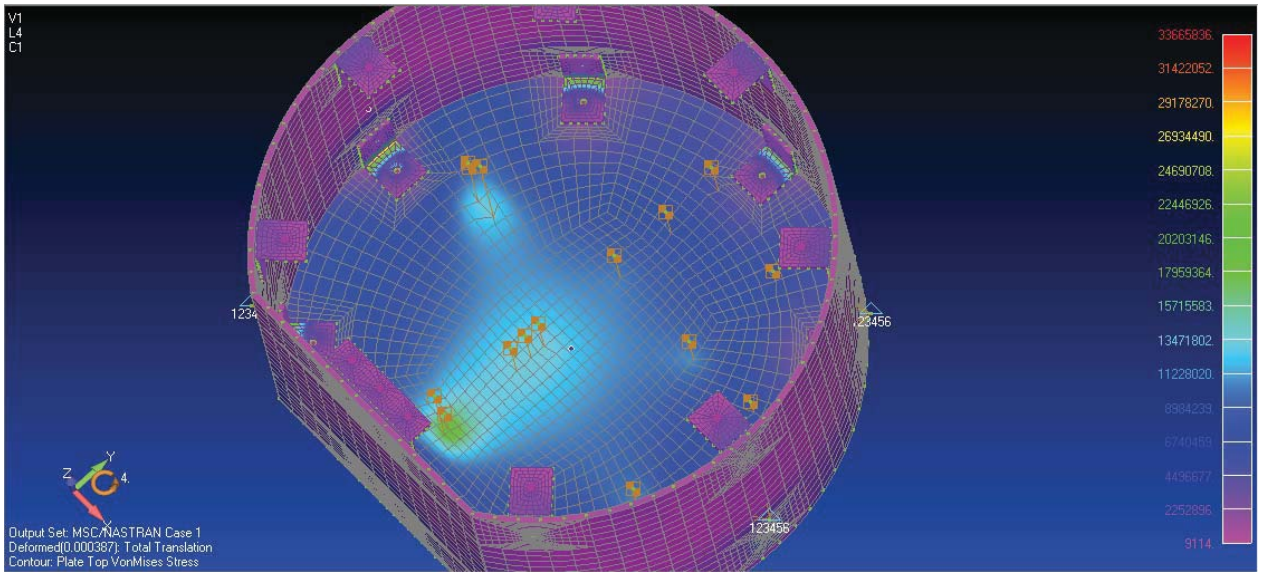

Figure 8. FEM of CWIS module without top plate (Contours of Von Mises stress)

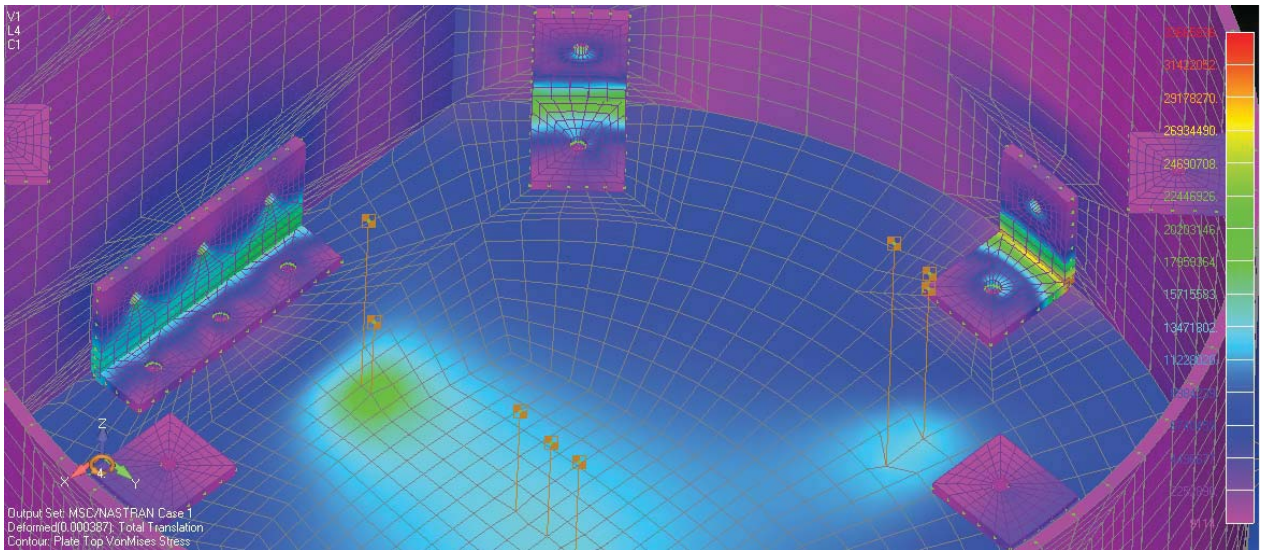

Figure 9. Closeup of CWIS module without top plate (Contours of Von Mises stress)

The results of the FEM analysis show that there will not be any critical deformations of the structural parts. We have a maximum translation on a L stiffner to the bottom plate of 0.38mm, and a maximum stress on the lateral skin near the first stiffener that attaches the bottom plate of M.S. 8.99.

The white noise for modal frequency response analysis was discretized in FEMAP, and then the excitation is simulated by a random vibration with a frequency of 20 kHz, as shown in figures 11-16.

In the following plot, each colour represents a connection node between the lateral skin and the damping springs around our module. The FEM results of the modal frequency response analysis are shown in the following figures. In all these figures, the horizontal axis is frequency, in Hz. In the Modal Frequency Response graphs, displacement is on the vertical axis.

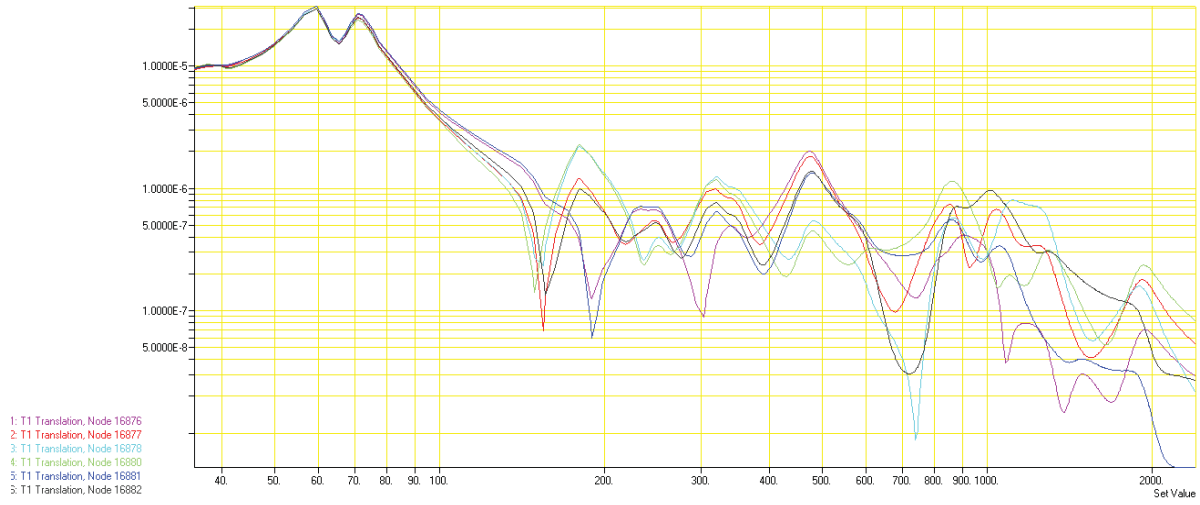

Figure 11. Modal Frequency Response Analysis – Displacement along X-axis.

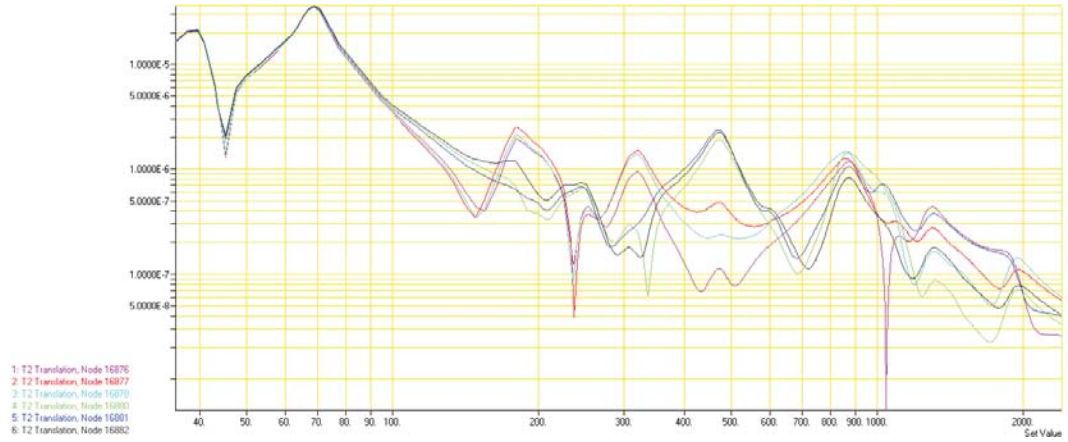

Figure 12. Modal Frequency Response Analysis – Displacement along Y-axis

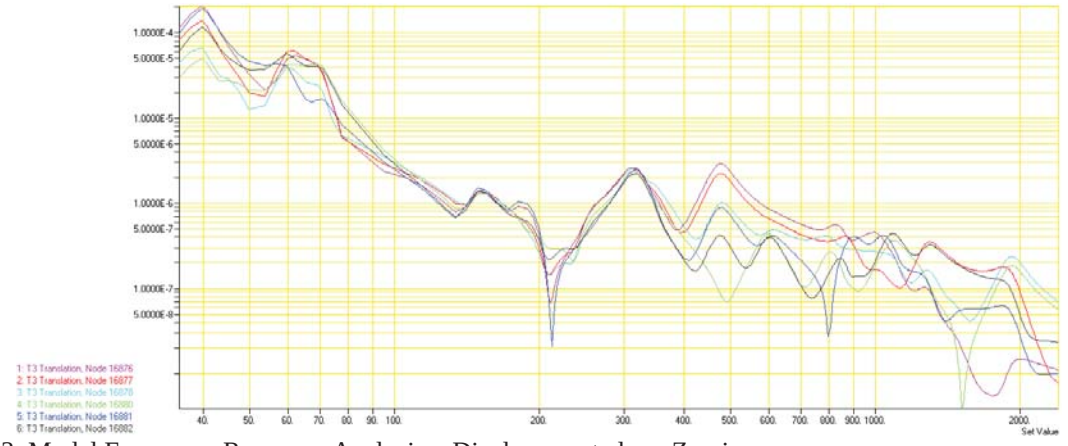

Figure 13. Modal Frequency Response Analysis – Displacement along Z-axis

The FEM results of the random response analysis are shown in Figures 14-16.

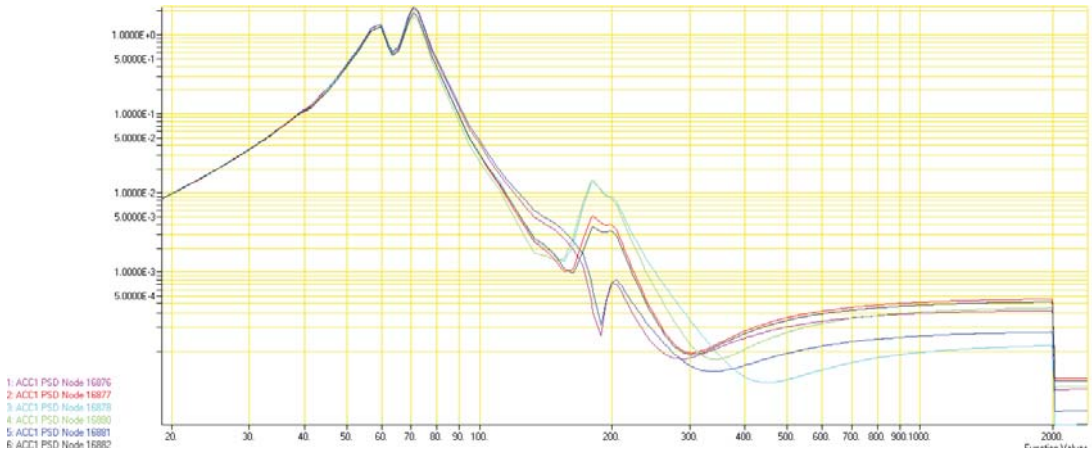

Figure 14. Random Response Analysis – Accelerations along X-axis

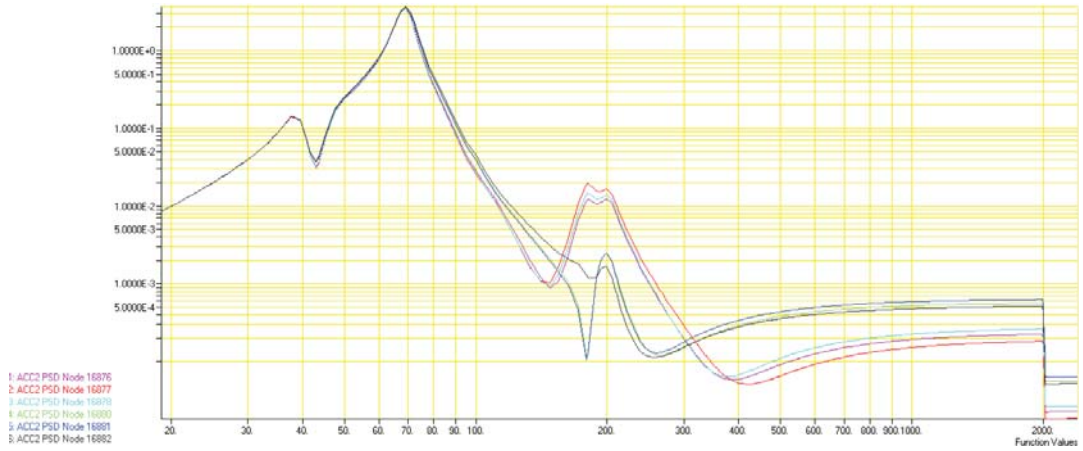

Figure 15. Random Response Analysis – Accelerations along Y-axis

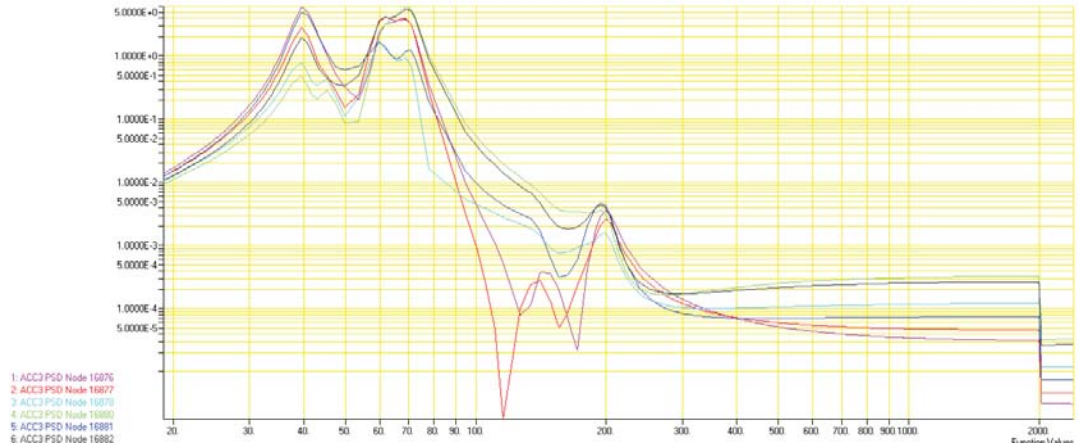

Figure 16. Random Response Analysis – Accelerations along Z-axis.

The modal and FEM analysis together indicate that the payload can stand up to the strenuous forces of launch and entry.

Thermal Systems

The liquid mixture must remain in the range of -13 to 90°C, to prevent a change of state. The camera and other electronics require even tighter thermal control. These can have functional problems outside a range of -10 to 60°C. At T-1h, the roof is removed from the launch site, and the rocket is elevated. The launch rules dictate that the experiment must be switched off at this point. Because the launch window is in early March, in northern Sweden, it is anticipated that outside temperatures could reach -30°C or below.

The experiment's main insulation is a 10mm thick layer of polyurethane foam in between our module's aluminium skin, and the skin of the rocket. Polyurethane is extremely versatile,[12] and has been used in a number of spacecraft applications, including on the space shuttle's external fuel tank.[6]

Thermal insulation built into our module will provide some protection, but not enough for this phase of the launch operations, especially if there is a hold during this period. As a result, hot air from an external source will be blown on our payload module to ensure that it stays above -10°C.

During the rocket flight, the outer structure of the rocket may reach 110°C at T+50s, due to heating from the motor. During re-entry, peak temperatures may reach 200°C.

Based on the physical dimensions, and the thermal conductivity (λ) of each of the materials, given in Table 2, a preliminary thermal analysis has been done.

	λ_i (W/mK)	Thickness (mm)	r_o (mm)	r_i (mm)
Rocket skin	210	4	178	174
Air gap	0.026	31	174	143
Module skin	210	3	143	140
Polyurethane	0.03	10	140	130

Table 2: Thermal characteristics of the outer body and insulation

The trends of internal temperature are plotted versus time in Figure 17.

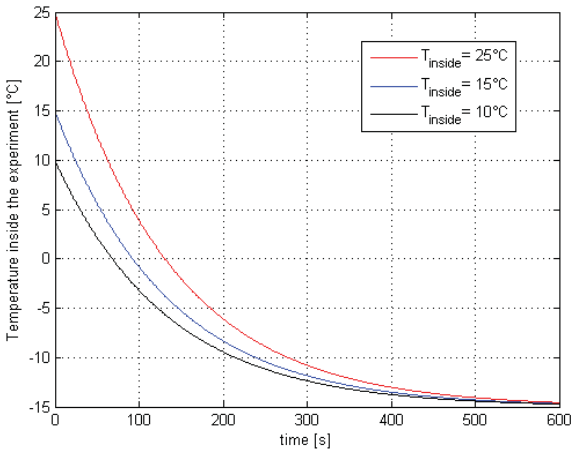

Figure 17. Thermal trends during rocket flight

This analysis is considered to be conservative, because the entire CWIS module was considered to be exposed to the outside temperature, when in fact only the sides are exposed to the outside atmosphere.

Electrical Systems

The CWIS experiment is supervised by a microcontroller that coordinates all the processes before and during the flight time. This microcontroller handles the temperature sensors, the state of the laser and the camera, the power of the heaters and the data storage activities. It also is responsible for the ground communication through the REXUS Service Module.

The experiment uses the power provided by the REXUS service module to power all of our electronic systems.

A DB15 connector is fixed to the optic plate and it's the only way to get power from the rocket. Other experiments' cables will pass between the rocket skin and the CWIS module, and they will be fixed to the D-SUB bracket. This configuration guarantees a distance between the experiment and the rocket module of about 21 mm, aligned to the D-SUB bracket.

The electrical system consists of two microcontrollers (one is the master that oversees all the operations in the experiment, the other one takes care of the data storage), one camera, two heaters, one laser and five thermocouples for monitoring the gradient and heater. The unregulated power coming from the RXSM is converted to 5V and 12V by two commercial DC/DC converters. Power consumption by the experiment varies during the flight due to the state of the systems; it ranges from a minimum of about 2W to a maximum of 20W. The time signals from the REXUS Service Module are used to trigger the experiment. These are LO, SODS, and SOE. During the rocket flight the CWIS Experiment uses the REXUS Service Module downlink to send collected housekeeping data (temperature, system status) to the ground station.

A schematic overview of the CWIS electronics layout is shown in Figure 18.

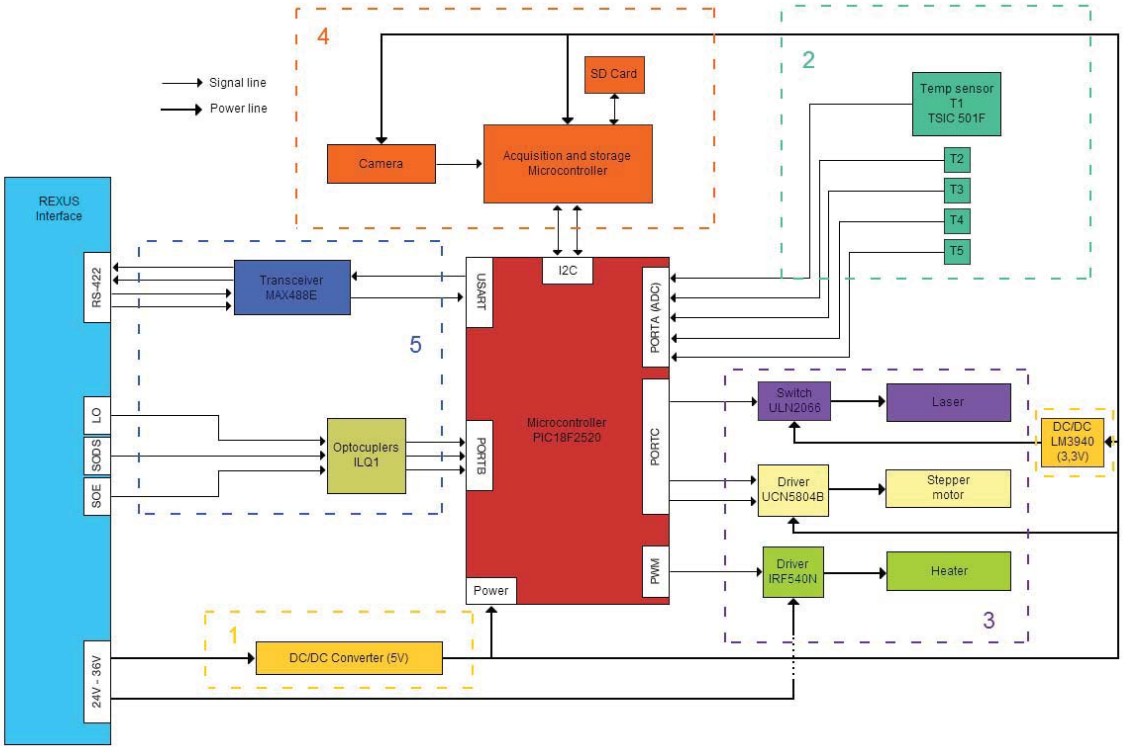

Figure 18. Electronics Schematic

Software Design

There are four distinct software development tasks associated with this project. First there are two software tools required onboard the rocket, in order to manipulate the onboard systems during the course of the flight. These are the main control board software, and the camera on-board data-handling (OBDH) software. Two pieces of software are also required on the ground. One is the mission control software, which allows for some manual control of the experiment, and also presents data from the downlink. Finally, there is the analytical software for fringe pattern analysis. Here we describe the main control board software and OBDH software. The general structure for this onbaord software is shown in Figure 19.

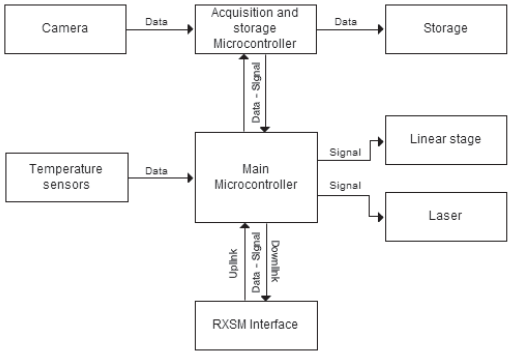

Figure 19. Software logic schematic

The main microcontroller handles the data in coming from the temperature sensors and drives the heating power and the laser power. It also manages the data that are sent both via the REXUS downlink and to the OBDH microcontroller for being stored in the SD card.

The program starts with the microcontroller power-on by the RXSM; it initializes the USART, I2C, ADC, PWM modules and the camera (stand-by). The program then starts the reading sequence from the temperature sensors and sends via downlink the values. At T-10, the microcontroller switches on the laser. When the "LO" signal occurs, when it receives the "SODS" signal the camera starts to record. On the "SOE" signal the duty cycle of the heater goes near 100% and heats the thermal mass and the phenomenon starts. After 232s the microcontroller switches off the camera, the heater and the laser and after 10 more seconds all systems may be turned off by a ground control command.

The camera acquisition software is developed under Linux using drivers provided by the camera manufacturer. The use of Linux is motivated by the existence of advanced drivers regarding storage drives operations. The acquisition software is written in C/C++ while file management will use bash scripts to easily copy files between memory locations using the standard UNIX file operations.

III. CONCLUSIONS

This paper presents the engineering design of the Chemical Waves in Soret Effect experiment currently being developed for the REXUS 16 launch campaign. Aside from the usual challenges of research, which are all present in abundance in this multidisciplinary project, there is the considerable challenge of the rocket launch. The accelerations, loadings, and mechanical and thermal issues associated with the launch include high-frequency vibrations, 20g accelerations, and transitions from far below freezing, to far above boiling temperatures. So far, our analyses indicate that the experiment will be able to perform as intended. A future work will detail the thorough testing of the assembled systems, and eventually, the data that is collected when the experiment is launched – currently scheduled for March of 2014.

IV. REFERENCES

1. Center, Manned Spacecraft. "Nonmetallic-Materials Development for Spacecraft Applications." *Conference on Materials for Improved Fire Safety*. Vol. 5096, P.88. National Aeronautics and Space Administration, Technology Utilization Office, 1971.
2. Dominguez, Gerardo, Gautam Wilkins, and Mark H. Thiemens. "The Soret effect and isotopic fractionation in high-temperature silicate melts." *Nature* 473.7345 (2011): 70-73.
3. Duhr, Stefan, and Dieter Braun. "Why molecules move along a temperature gradient." *Proceedings of the National Academy of Sciences* 103.52 (2006): 19678-19682.
4. Eslamian, M., Advances in Thermodiffusion and Thermophoresis (Soret Effect) in liquid mixtures, Frontiers in Heat and Mass Transfer 2 (2011)
5. EuroLaunch, REXUS User Manual
6. Facts, N. A. S. A. *Thermal Protection System*. NASA Report FS-2004-08-97 MSFC, NASA Marshall Space Flight Center, Huntsville, AL, 2004.
7. Geelhoed, P. F., R. Lindken, and J. Westerweel. "Thermophoretic separation in microfluidics." *Chemical Engineering Research and Design* 84.5 (2006): 370-373.
8. "Guideline for Use of Fizeau Interferometer in Optical Testing." NASA, n.d. Web. 15 Aug. 2013. <http://engineer.jpl.nasa.gov/practices/2404.pdf>.
9. James, John T. "Ethylene glycol." *Spacecraft Water Exposure Guidelines for Selected Airborne Contaminants* 3 (2008): 86-125.

10. Oreb, Bozenko F., et al. "Interferometric measurement of refractive index inhomogeneity on polished sapphire substrates: application to LIGO-II." *International Symposium on Optical Science and Technology*. International Society for Optics and Photonics, 2001.

11. Van Vaerenbergh, S. - Legros J.C., Kinetics of the Soret Effect: Transient in the Transport Process, Physical Review A 41.12 (1990)

12. Wang, Linda. "Polyurethane Foam." *Chemical and Engineering News* 84.2 (2006): 48.